Ground-state nuclear g factor of ^{97}Ru

K. Leuthold, E. Hagn, H. Ernst, and E. Zech
Physik-Department, Technische Universität München, D-8046 Garching, West Germany
(Received 15 June 1979)

The magnetic hyperfine splitting constant $g\mu_N H_{HF}/h$ of ^{97}Ru as a dilute impurity in Fe has been determined by the technique of nuclear magnetic resonance on oriented nuclei to be 117.69 ± 0.02 MHz. With the known hyperfine field for Ru*Fe* of -504 ± 12 kG the ground-state nuclear g factor of ^{97}Ru is deduced to be $(-)0.306 \pm 0.008$. The resonance shift and the spin-lattice-relaxation time have been measured as functions of an external magnetic field.

[RADIOACTIVITY ^{97}Ru from ^{96}Ru(n,γ); NMR on oriented nuclei. Deduced μ, Knight shift, relaxation times.]

I. INTRODUCTION

The deviations of nuclear magnetic moments from the single-particle Schmidt values are qualitatively well understood for nuclear states with configurations of few nucleons outside of closed shells. The main deviations are believed to be due to $j^\pi = 1^+$ polarization of the core[1,2] and, in addition, to mesonic effects.[3,4] In the region $A \sim 90$, where $^{90}_{40}Zr_{50}$ or $^{88}_{38}Sr_{50}$ are assumed to be fairly good magic nuclei, the states with few protons in the $g_{9/2}$ shell and few neutrons in the $d_{5/2}$ shell are well suited for systematic studies of these effects. Most experiments have been done for a better understanding of the $\pi g_{9/2}$ magnetic moments, which have shown that the additivity of magnetic moments is violated, and that an anomalous orbital magnetism due to mesonic effects exists.[5-7] For the interpretation of the data from odd-odd nuclei, precise data for the neutron contributions to the magnetic moments have to be available. In this context, a systematic study of $d_{5/2}$ neutron magnetic moments is of interest.

In addition to these aspects the magnetic moments of ruthenium nuclei are interesting for the following reason. The ground-state spin of the lighter isotopes ^{95,97,99,101}Ru is $j^\pi = \frac{5}{2}^+$, which can be understood as a pure $d_{5/2}$ shell model configuration. The ground-state spins of the heavier isotopes ^{103}Ru and ^{105}Ru have not been determined experimentally in a direct way. From indirect arguments, however, the most probable assignment is $j^\pi = \frac{3}{2}^+$, which could be understood in the frame of the shell model as a $(d_{5/2})^3_{3/2^+}$ configuration. A measurement of the magnetic moments could possibly yield some information on this subject. First nuclear orientation experiments on ^{97}Ru*Fe*, ^{103}Ru*Fe*, and ^{105}Ru*Fe* (Ref. 8) showed, however, that the γ anisotropies of ^{103}Ru and ^{105}Ru are very small, so that no unique conclusions could be drawn. A combination of the nuclear orientation (NO) measurements with NMR-ON experiments (nuclear magnetic resonance on oriented nuclei detected by the anisotropy of radiation), however, would yield a precise value for the nuclear g factors and would thus allow a *unique* spin determination. (This feature is based on the fact that the NO method yields the magnetic moment μ, while the NMR-ON method yields the g factor.) In order to clarify whether the NMR-ON method is well applicable to Ru*Fe* systems, the first experiments have been performed on ^{97}Ru*Fe* for which the γ anisotropy is comparatively large. These experiments are described in this paper.

II. PRINCIPLE OF MEASUREMENT

A. Nuclear orientation

The angular distribution of oriented nuclei is most conveniently written as[9]

$$W(\Theta) = 1 + \sum_{k=2,4} U_k F_k B_k^{(j)}(gB/kT) P_k(\cos\Theta) Q_k . \tag{1}$$

The different coefficients have the following meaning. The F_k are the usual angular correlation coefficients, and the U_k take into account the deorienting effect of preceding unobserved (γ, $\beta^\pm$, EC) transitions. The U_k and F_k depend on the parameters of the nuclear decay, i.e., on spins, multipolarities, and mixing ratios of different multipolarities if the transitions are not pure. The B_k describe the degree of orientation of the initial state. They depend on gB/kT and on the spin j of the state. If the B_k are calculated as a function of $\mu B/kT$ instead of gB/kT, it is found, that the j dependence of B_k is rather weak in the region $gB/kT < 1$. This has the consequence that μ can be determined rather reliably, even if no unique spin assignment is possible. (The asymp-

totic values $\bar{B}_k^{(j)}$, which are obtained for $gB/kT \gg 1$, depend, of course, on j). The temperatures which are necessary for the corresponding saturation of the anisotropy are extremely low in most cases and cannot be obtained in most NO experiments. The $P_k(\cos\Theta)$ in formula (1) are Legendre polynomials, Θ being the angle between the quantization axis, which, in the present case of pure magnetic interaction, coincides with the direction of the magnetic field, and the direction of observation. The Q_k take into account the solid angle of the detectors, they are normally in the region near unity. The sum in formula (1) runs on even k only, the maximum value $k_{\max}$ depending on the spins and multipolarities which are involved in the decay cascade. It is in most cases given by $k_{\max}=4$.

To get a considerable degree of orientation at $T\sim 10$ mK, magnetic fields of the order of >100 kG are necessary. This is obtained by utilizing the internal hyperfine fields B_{HF}, which act on dilute impurities in ferromagnetic host lattices (Fe, Co, Ni, Gd). The value of B_{HF} is dependent on the type of impurity-host system; a compilation of most presently known hyperfine fields is given in Ref. 10.

To get rid of several disturbing effects, such as the decrease of the counting rate due to the finite lifetime of the parent nucleus, the ratio

$$\epsilon=\frac{W(0)}{W(90)}-1 \tag{2}$$

is normally calculated and analyzed as a function of the temperature T.

The precision to which magnetic moments can be determined from the temperature dependence of the γ anisotropy depends strongly on the particular case, a typical value being ~5%. Some limiting factors are imprecisely known mixing ratios of different tensor ranks of the preceding $\beta^{\pm}$ or EC transitions, nonalignment of the hyperfine field (Aharoni effect), different spin-lattice-relaxation times in comparison to those of the thermometers, etc. A very much higher precision is obtainable with the NMR-ON method which is described in the next subsection.

B. Fast-sweep nuclear magnetic resonance on oriented nuclei

In the NMR-ON method[11] the γ anisotropy is used as a detector for nuclear magnetic resonance. As a precise knowledge of the absolute value of the γ anisotropy is not necessary, an accurate determination of the temperature of the sample is also not necessary. The only restriction is that the γ anisotropy is so large that the resonant destruction can be observed. The resonance condition is given by

$$h\nu=g\mu_N[B_{\mathrm{HF}}+(1+K)B_0]\,, \tag{3}$$

where g is the nuclear g factor, μ_N the nuclear magneton, B_{HF} the magnetic hyperfine field, K the Knight shift, and B_0 the external magnetic field, which is necessary to orient the ferromagnetic domains, and which thus establishes a unique quantization direction with respect to which the γ anisotropy is observed. If the Knight shift can be neglected, formula (3) reduces to

$$h\nu=g\mu_N(B_{\mathrm{HF}}+B_0)\,. \tag{4}$$

In this case the nuclear g factor can be determined from the resonance shift with the external field, i.e., without the knowledge of B_{HF}.

Besides the static resonance condition, which is given by formula (3), dynamic effects have to be considered in the experiment. The rf field, which has the "correct" frequency ν_0, induces rf transitions between the m sublevels, the effect being a total or at least partial destruction of the polarization with the corresponding change in the γ anisotropy. If the rf field is now switched off, the system returns to the thermal equilibrium with a characteristic time constant T_1'. This time constant, which is normally denoted as spin-lattice-relaxation time, is not uniquely defined as will be shown in the following. The spin-lattice-relaxation mechanism can be described by a set of rate equations for the sublevel populations, the essential parameter being a reduced matrix element which describes the strength of the coupling between the nuclei and the lattice.[12] In the high-temperature region $kT\gg gB$, the rate equations can be solved analytically. In this approach, the polarization, and all physical quantities which are proportional to it such as the magnetization, decay exponentially to the equilibrium value, the time constant being the spin-lattice-relaxation time T_1 which follows the Korringa law $T_1T=\mathcal{K}$, where $\mathcal{K}$ is the Korringa constant. In the low-temperature region $kT\ll gB$, and also in the region of intermediate temperature $kT\approx gB$, the rate equations have to be solved numerically. The time dependence of the polarization or the alignment consists of a sum of exponential functions with different time constants. It is found, however, that the return of the γ anisotropy to the equilibrium value can be described in a fairly good approximation by a single-exponential decay with a time constant T_1', which is different from the above T_1 and, in addition, which is dependent on the initial conditions, i.e., on the deviation of the system from the thermal equilibrium. This means, however, that a proportionality holds be-

tween T_1 and T_1', the proportionality constant being fixed if the temperature and the deviation from the equilibrium are kept constant. Thus, a functional dependence of T_1 on any parameter, such as the external magnetic field, can be detected by observing the corresponding dependence of T_1', which can be measured more easily.

The resonance frequency ν_R and the relaxation time constant T_1' can be measured *simultaneously* if a sweep-mode technique for the applied rf field is used. This nonconventional technique will be described in the following. The main features are shown in Fig. 1. Starting at $\nu=\nu_1<\nu_R$ the frequency of the applied rf field is swept continuously over the resonance with a constant sweep rate $d\nu/dt=+\rho$. At $\nu=\nu_2>\nu_R$ the sweep direction is reversed, the rf frequency is swept continuously over the resonance again, the sweep rate being now $d\nu/dt=-\rho$. At $\nu=\nu_1$ the sweep direction is reversed again, initiating a new cycle. This is shown in the lower part of Fig. 1. Before discussing the response of the nuclear spin system, the effect of inhomogeneous broadening has to be considered. It is found experimentally that the hyperfine field does not have a sharp value but a certain distribution. Assuming a Gaussian shape, which is a good approximation in most cases, the distribution of the resonance around the center frequency ν_R is given by

$$G(\nu)=f\left(\frac{\ln 2}{\pi}\right)^{1/2}\frac{1}{\Gamma_0}\exp[-\ln 2(\nu-\nu_R)^2/\Gamma_0^2]\,, \quad (5)$$

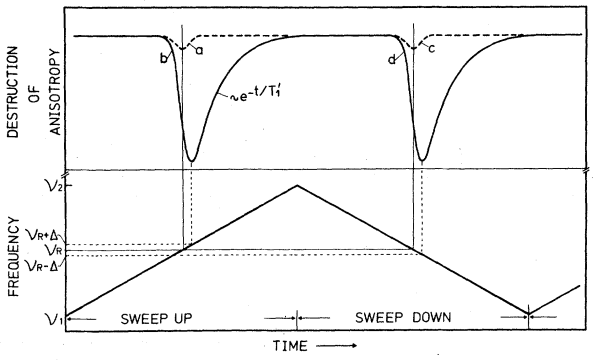

FIG. 1. Details of the sweep-mode technique for NMR-ON measurements. The rf center frequency is swept continuously up and down between the boundary frequencies ν_1 and ν_2 with a constant sweep rate $d\nu/dt=\pm\rho$ (bottom). The response of the γ anisotropy (top) depends on the choice of the sweep velocity (see text). In the adiabatic case, two symmetric resonances with the same center at ν_R are observed (curves a and c). In the nonadiabatic case, an integrating effect is active which leads to asymmetric resonances with a shift of the center and an exponential decay in sweep direction (curves b and d).

where Γ_0 is the inhomogeneous linewidth and f is the fraction of nuclei which can be affected by the rf. The normalization is chosen in such a way that

$$\int G(\nu)d\nu=f \quad (6)$$

is given. In the ideal case, $f=1$ is expected. To get a reasonable resonance effect, the rf field has to be frequency modulated. Assuming that all time-dependent effects can be neglected the observed resonance effect at a frequency ν is then given by

$$R_a(\nu)=\int_{\nu-\Delta f}^{\nu+\Delta f} G(\nu')d\nu'\,, \quad (7)$$

where Δf is the modulation width, and a stands for adiabatic approximation. If Δf is small in comparison to Γ_0 the shape of $R_a(\nu)$ is approximately Gaussian again, the linewidth and the amplitude being dependent on the value of Δf. For a precise determination of ν_R, the modulation width Δf has to be chosen properly as a compromise between a large resonance effect and a small resonance linewidth.

If the resonances are measured with a sweep-mode technique the time-dependent effects of the spin-lattice relaxation have to be taken into account. The resonance effect is then given by

$$R(\nu)=R_a(\nu)+\int_{\nu_0}^{\nu} R_a(\nu')\exp\{-[t(\nu)-t'(\nu')]/T_1'\}d\nu'\,. \quad (8)$$

The second term describes the resonance effect obtained at earlier times, which is decaying with the anisotropy relaxation time. The far-off-resonance frequency ν_0 is either ν_1 or ν_2 (see Fig. 1) for the upward or downward sweep direction, respectively. If we introduce the time during which a frequency interval Γ_0 is passed,

$$\tau=\int_{-\Gamma_0/2}^{\Gamma_0/2}(d\nu/dt)^{-1}\,dt=\frac{\Gamma_0}{d\nu/dt}\,. \quad (9)$$

Formula (8) can be written as

$$R(\nu)=R_a(\nu)+\int_{\nu_1}^{\nu} R_a(\nu')\exp\left(-\frac{\nu-\nu'}{\Gamma_0}\frac{\tau}{T_1'}\right)d\nu' \quad (10a)$$

for the sweep up and

$$R(\nu)=R_a(\nu)-\int_{\nu_2}^{\nu} R_a(\nu')\exp\left(-\frac{\nu'-\nu}{\Gamma_0}\frac{\tau}{T_1'}\right)d\nu' \quad (10b)$$

for the sweep down. This shows that an asymmetry of $R(\nu)$ is introduced, depending on the sweep direction, the essential asymmetry parameter being τ/T_1', i.e., the (experimentally choosable) sweep velocity. In the slow-sweep limit

$\tau/T_1' \gg 1$, $R(\nu)$ reduces to the "adiabatic" case $R_a(\nu)$. This is illustrated by the curves *a* and *c* of Fig. 1. Both resonances have the same center frequency ν_R. In the ultrafast limit $\tau/T_1' \ll 1$, the structure of $R(\nu)$ would be that of the error function. In this case all information on T_1' would be lost, too.

For $\tau/T_1' \approx 1$, the measured resonance effect $R(\nu)$ has an asymmetric shape, with an exponential decay in sweep direction. This is illustrated in Fig. 1 (curves *b* and *d*). Moreover, the "center" frequency (the frequency at which the destruction of the anisotropy has its maximum value) is shifted to $\nu_R + \Delta$ or to $\nu_R - \Delta$, depending on the sweep direction. For the determination of ν_R from slow-sweep mode measurements, where Δ is small, but not negligible, an equal number of spectra with opposite sweep direction are usually added together. With this procedure the observed linewidth is slightly increased, but the center frequency, which is the main result, is not affected by the sweeping. Because of the integrating effect of the fast-sweep technique, the rf modulation width can be chosen small, allowing a highly precise determination of ν_R. Moreover, the relaxation time T_1' can be determined simultaneously.

In the presence of a small quadrupole interaction, which may be superimposed to the magnetic hyperfine splitting, deviations of the observed resonance behavior from that given by formula (7) are expected. The main effect results then in the (observable) fact that the resonance amplitudes are different for both sweep directions. Conversely, if these amplitudes are found to be equal, one can conclude that quadrupole effects have not to be considered in the determination of the magnetic hyperfine splitting constant from the observed resonance frequency.

III. EXPERIMENTAL DETAILS

The ^{97}Ru*Fe* samples were prepared in the following way. Inactive ^{96}Ru*Fe* alloys were produced by melting isotopically enriched ^{96}Ru (enrichment 98.1%) with highly pure iron (purity >99.999%) in an electron beam furnace. For the concentration of ^{96}Ru the relatively high value of 1 at % was chosen because of the small neutron capture cross section of $\sigma \sim 0.3$ b. The alloys were cold rolled with intermediate annealing steps until a final thickness of ~2 μm was reached. Foils with an area of 8×8 mm^2 were irradiated at the Karlsruhe research reactor FR2 for five days in a neutron flux of $\phi = 10^{14}$ n/sec cm^2 to produce the radioactive isotope ^{97}Ru ($T_{1/2} = 2.9$ d; $j^\pi = \frac{5}{2}^+$). After the irradiation the foils were annealed again at a temperature of ~700 °C under high-vacuum atmosphere (~10^{-7} torr). Special care was taken in slowly cooling down the samples to room temperature. Two foils were then soldered with Ga-In solder, which has the low melting point of 15 °C, to both sides of the Cu coldfinger of a demagnetization cryostat. With Cr-K alum as cooling salt, the samples were cooled to a temperature of ~0.01 K. To orient the ferromagnetic domains a small external magnetic field (<7 kG), which was provided by superconducting split coils, was applied in a direction parallel to the foil plane. The γ radiation was analyzed with four 7.6 cm diam × 7.6 cm NaI(Tl) detectors which were placed at 0°, 90°, 180°, and 270° with respect to the direction of the magnetic field.

The rf field was applied using a one-turn coil, the direction being perpendicular to the static field and parallel to the foil plane. The constant frequency sweep was achieved by driving the mechanical tuning of the rf oscillator with a stepping motor. Using different gearing units, the sweep rate $d\nu/dt$ could be varied over a large range. In comparison to electrically tuned oscillators this method has the advantage of a very much better constancy of the sweep rate. The rf field was frequency modulated with a modulation width of 100 kHz and a modulation frequency of 1 kHz. The output of the oscillator was measured continuously using a high-precision frequency counter operating with a repetition rate of 1 kHz. The frequency modulation of the oscillator was synchronized with the frequency counter. Thus a unique determination of the effective center frequency is possible, independent of the modulation width. The output of the frequency counter was used to synchronize a multichannel analyzer, which operated in multiscaling mode.

IV. RESULTS

In the decay of ^{97}Ru only one strong γ transition with an energy of 216 keV is present. A simplified decay scheme is illustrated in Fig. 2. For ^{97}Ru*Fe*,

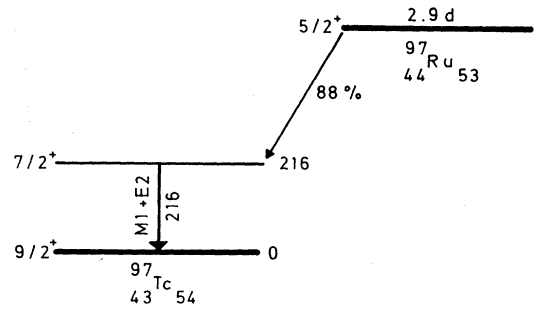

FIG. 2. Simplified decay scheme of ^{97}Ru.

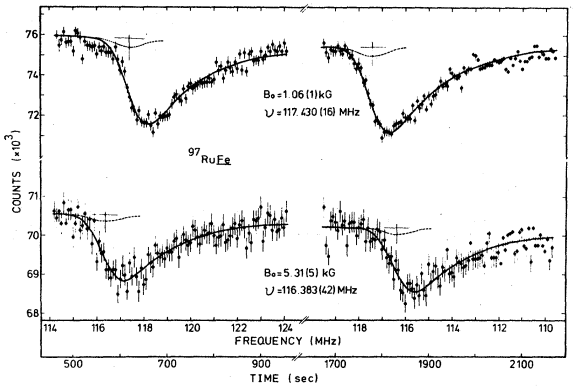

FIG. 3. Fast-sweep-NMR-ON resonances for two different values of the polarizing field B_0. The scale of the abscissa is a time scale (bottom) which has been converted to frequency (top). The left-hand resonances have been measured during the sweep up, the right-hand resonances during the sweep down. The dashed curves are the "adiabatic" resonances as obtained from the least-squares fit utilizing Eq. (10).

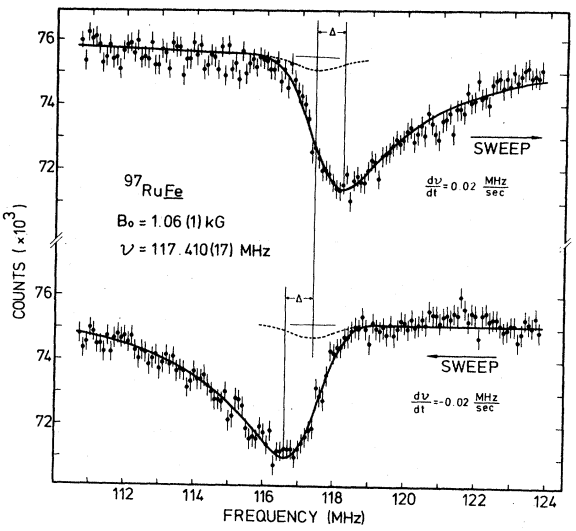

FIG. 4. Details of a fast-sweep-NMR-ON resonance run for $B_0 = 1.06$ (1) kG versus frequency. The maxima of the resonance curves are clearly shifted by $\Delta = 0.80$ MHz in sweep direction (upper spectrum: sweep up; lower spectrum: sweep down). The full curves are the results of a least-squares fit utilizing Eq. (10); the dashed curves are the "adiabatic" resonance, which is also a result of the fit.

the corresponding γ-ray anisotropy is $\epsilon \sim 20\%$ at $T \sim 10$ mK. Figure 3 shows resonance spectra, measured at 0° (with respect to B_0) for two different values of the external magnetic field. The solid curves are the results of least-squares fits, utilizing Eq. (10) as theoretical curve and a Gaussian line shape for the inhomogeneous broadening. The dashed curves in Fig. 3 are the "adiabatic" resonances, which have been added to demonstrate the large enhancement of the observed resonance effect by the fast-sweep technique. The shift of the resonance towards smaller frequencies with increasing polarization field is due to the negative sign of the hyperfine field. More details of the resonance spectra for a measurement with $B_0 = 1.06(1)$ kG can be seen in Fig. 4. It is clearly demonstrated that the maximum of the resonance destruction is shifted by $\Delta = 0.8$ MHz in sweep direction. Thus a folding of both spectra to get rid of the asymmetric line shape would not be a good procedure for the precise determination of ν_R. The upper part of Fig. 5 shows the resonance frequencies as a function of the external magnetic field. The solid line is the result of a least-squares fit, which yields

$$g\mu_N B_{HF}/h = 117.69(2) \text{ MHz}$$

for the hyperfine splitting and

$$g\mu_N(1+K)/h = 0.246(3) \text{ MHz/kG}$$

for the resonance shift. The lower part of Fig. 5 illustrates the deviation of the measured points from the fitted line, thus demonstrating the good accuracy obtainable with the fast-sweep technique. The quoted error for the resonance shift is mostly

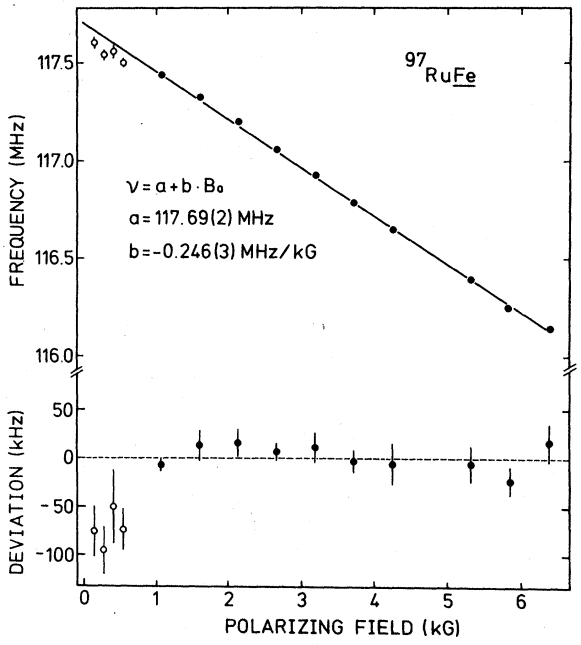

FIG. 5. NMR-ON center frequencies (top) and deviation of these frequencies from the fitted straight line (bottom). The values for $B_0 < 1$ kG have been added for demonstration; they are not used for the fit of the resonance shift because of the incomplete magnetic saturation of the samples in this region.

due to an (absolute) uncertainty of ~1% in the calibration of the external magnetic field. This calibration has been performed by measuring the resonance shift of ^{60}Co*Fe*, which was found to be reproducible within an accuracy of ~1%.

For the interpretation of our hyperfine splitting, the knowledge of the hyperfine field for Ru*Fe* is necessary. From Mössbauer-effect measurements on ^{99}Ru*Fe* (Ref. 13) the splitting of the $\frac{3}{2}^+$ state at 90 keV has been measured as $\nu_M = 72.8(1.3)$ MHz. With the known magnetic moment of $\mu_{3/2} = -0.284$ (6) μ_N (Ref. 14) for this $\frac{3}{2}^+$ state, $B_{HF} = -504(14)$ kG is calculated. (The negative sign has been measured with the use of an external magnetic field.)[13] From NMR investigations of ^{99}Ru and ^{101}Ru as impurities in Fe, Co, and Ni (Ref. 15) the ground-state splitting of ^{99}Ru*Fe* (1 at %) has been found to be $\nu_M = 95.75(10)$ MHz. With $\mu_{5/2} = -0.623(19)$ μ_N the corresponding hyperfine field is deduced to be $B_{HF} = -504(15)$ kG. These two values are not completely independent, however, as $\mu_{5/2}$ is calculated using $\mu_{3/2}$ and the measured g-factor ratio $g_{3/2}/g_{5/2} = 0.759(16)$.[13] Thus,

$$B_{HF} = -504(12) \text{ kG}$$

[instead of the usual tabular value of −500 (10) kG (Ref. 10)] is adopted to deduce the ground-state g factor of ^{97}Ru, which yields

$$|g| = 0.306(8).$$

Much more precise results are obtained for the ratios of the ground-state g factors of ^{97}Ru, ^{99}Ru, and ^{101}Ru. These, together with the resonance frequencies, are compiled in Table I.

From the resonance shift we get

$$|g(1+K)| = 0.315(7),$$

which can be used to deduce the value

$$K = +2.9(3.4)\%$$

for the Knight shift of ^{97}Ru*Fe*. This value, which is consistent with $K = 0$, lies well within the usual range of Knight shifts for dilute iron host alloys[16,17] in the mass region $A < 100$.

Figure 6 shows the linewidth (bottom), the resonance effect (middle), and the anisotropy relaxation time T_1' (top) as a function of the external magnetic field B_0. The linewidth is found to be rather constant in the whole range. This behavior is quite normal, the mean value $\Gamma = 1.4(2)$ MHz is, however, relatively large in comparison to other NMR-ON data on other systems in this frequency range. This could be caused by the relatively high Ru concentration of ~1 at.%, which had to be chosen because of the small neutron capture cross section of ^{96}Ru.

The dependence of the resonance effect on B_0 can be understood easily: The increase between $B_0 = 0$ and $B_0 = 1$ kG is due to the increasing degree of orientation, which reaches the saturation value at ~1 kG. [In this region of incomplete saturation the measured center frequencies are not described properly by Eq. (3) because of the finite angle between B_0 and B_{HF}, which, in addition, depends on B_0. Thus the resonance frequencies for $B_0 < 1$ kG have been omitted for the analysis of the hyperfine

TABLE I. Magnetic hyperfine splitting and ratios of ground-state g factors of ^{97,99,101}Ru.

System	ν_M(MHz)	g/g (^{97}Ru)[a]	Reference
^{97}Ru*Fe*	117.69(2)	1.0	b
^{99}Ru*Fe*	95.75(10)	0.8136(8)	c
^{101}Ru*Fe*	107.30(10)	0.9117(8)	c

[a] Possible hyperfine anomalies are neglected in this ratio. This is possible, as only differences of hyperfine anomalies would enter, which are expected to be smaller than the quoted error.

[b] This work.

[c] J. J. Murphy, T. J. Burch, and J. I. Budnick, J. Phys. Soc. Jpn. 36, 634 (1974).

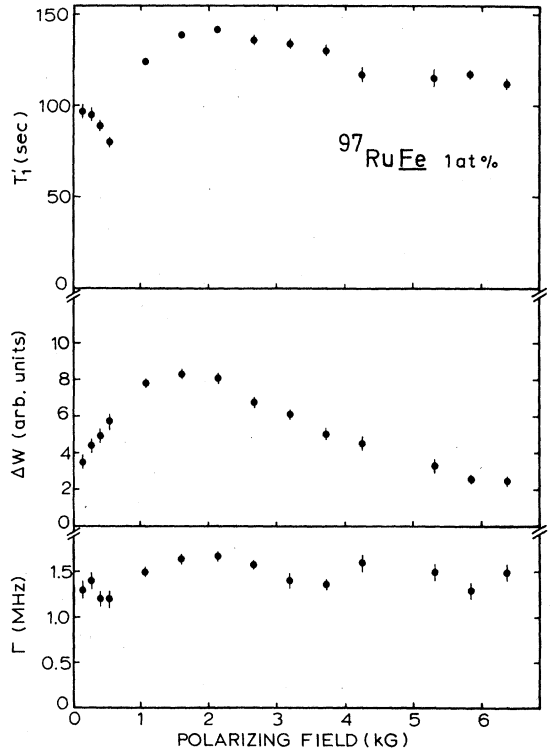

FIG. 6. Observed linewidth (bottom), resonance effect (middle), and anisotropy relaxation time (top) versus the applied external magnetic field.

splitting and the resonance shift.] The decrease of the resonance effect for $B_0 > 1.5$ kG is probably due to the decreasing enhancement factor for the rf field, which is proportional to B_{HF}/B_0 in first approximation.

The behavior of the relaxation time T_1' in dependence of B_0 is anomalous in comparison to that of other systems in this mass region. Neglecting the data points for the magnetization region $B_0 < 1$ kG, T_1' is found to be rather constant, with a slightly decreasing trend for $B_0 > 2$ kG. This decrease is partly caused by the smaller deviation of the sublevel populations from the equilibrium value, as observed by the decreasing resonance effect. An increase of T_1' by a factor ~5 between 0 and 5 kG, as observed, e.g., on ^{90}NbFe and ^{94}TcFe,[18] is clearly not present for ^{97}RuFe.

TABLE II. Magnetic moments of neutron $\frac{5}{2}^+$ states in the mass region $A > 90$.

Isotope	μ (μ_N)	Reference
$^{91}_{40}Zr_{51}$	−1.30362(2)	a
$^{93}_{42}Mo_{51}$	−1.20(5)	b
$^{95}_{42}Mo_{53}$	−0.9142(1)	c
$^{97}_{42}Mo_{55}$	−0.9335(1)	c
$^{97}_{44}Ru_{53}$	−0.765(20)	d
$^{99}_{44}Ru_{55}$	−0.623(19)	e
$^{101}_{44}Ru_{57}$	−0.698(24)	f
$^{105}_{46}Pd_{59}$	−0.642(3)	g
$^{105}_{48}Cd_{57}$	−0.7393(2)	h
$^{107}_{48}Cd_{59}$	−0.615055(1)	j,k
$^{109}_{48}Cd_{61}$	−0.827846(1)	j,l
$^{111}_{48}Cd_{63}$	−0.7656(25)	m

[a] E. Brun, J. Oeser, and H. H. Staub, Phys. Rev. 105, 1929 (1957).

[b] E. Hagn, E. Zech, and G. Eska, Hyp. Int. 4, 201 (1978).

[c] W. G. Proctor and F. C. Yu, Phys. Rev. 81, 20 (1951).

[d] This work.

[e] E. Matthias, S. S. Rosenblum, and D. A. Shirley, Phys. Rev. 139, B532 (1965).

[f] J. J. Murphy, T. J. Burch, and J. I. Budnick, J. Phys. Soc. Jpn. 36, 634 (1974).

[g] J. A. Seitchik, A. C. Gossard, and V. Jaccarino, Phys. Rev. 136, A1119 (1964).

[h] N. S. Laulainen and M. N. McDermott, Phys. Rev. 177, 1615 (1969).

[j] P. W. Spence and M. N. McDermott, Phys. Lett. 42A, 273 (1972).

[k] F. W. Byron, Jr., M. N. McDermott, and R. Novick, Phys. Rev. 132, 1181 (1963).

[l] M. N. McDermott and R. Novick, Phys. Rev. 131, 707 (1963).

[m] H. Bertschat, H. Haas, F. Pleiter, E. Recknagel, E. Schlodder, and B. Spellmeyer, Z. Phys. 270, 203 (1974).

V. DISCUSSION

With $j^\pi = \frac{5}{2}^+$, the magnetic moment of ^{97}Ru is found to be

$$\mu = (-)0.765(20)\ \mu_N .$$

The negative sign has been adopted from the systematics of magnetic moments of $\frac{5}{2}^+$ states in this mass region. A compilation of magnetic moments of $\frac{5}{2}^+$ states is given in Table II for the mass region $A > 90$, where the neutron $d_{5/2}$ shell is successively filled. With the exception of ^{111}Cd, all data originate from measurements on ground states. The value for $^{93}_{51}Mo_{42}$ has been deduced in the following way: Assuming $^{92}_{50}Mo_{42}$ to be the "core," the isotopes $^{93}_{51}Mo_{42}$, $^{93}_{50}Tc_{43}$, and $^{94}_{51}Tc_{43}$ have the configurations $|\nu d_{5/2}\rangle$, $|\pi g_{9/2}\rangle$, and $|\nu d_{5/2}\pi g_{9/2}\rangle_{7^+}$. As the magnetic moments of ^{93}Tc and ^{94}Tc are known,[19] the neutron contribution to the magnetic moment of ^{94}Tc can be calculated:

$$\mu(\nu d_{5/2}) = \mu(7^+) - \mu(\pi g_{9/2}) .$$

This procedure is based on the assumption that the magnetic moments of the one-particle states remain unchanged for the two-particle state, which is valid in most cases to an accuracy of several percent. Figure 7 illustrates the behavior of the $d_{5/2}$ neutron magnetic moments versus the neutron number. The relatively large values for $N = 51$ are quite normal for states with one particle outside closed shells. The strong deviation from

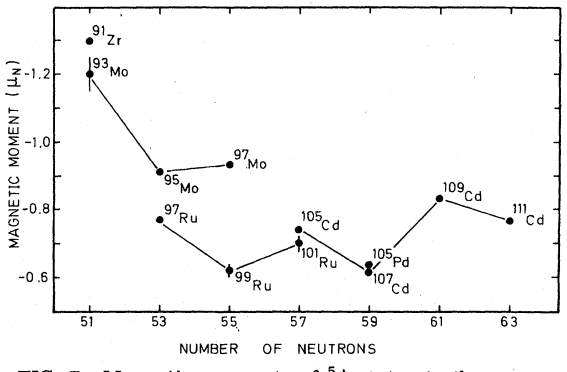

FIG. 7. Magnetic moments of $\frac{5}{2}^+$ states in the mass region $A > 90$ versus neutron number. A similar structure of μ for ^{93,95,97}Mo, ^{97,99,101}Ru, and ^{105,107,109}Cd can be seen. This yields a strong evidence for the fact that the addition of proton pairs in the $\pi g_{9/2}$ shell, by going from Mo to Cd, is accompanied by a simultaneous addition of the same number of neutron pairs into the $\nu g_{7/2}$ shell.

TABLE III. Calculated magnetic moments of $\frac{5}{2}^+$ states for different neutron configurations.

Nucleus	Proton configuration [a]	Neutron configuration [a]	μ_{cal} (μ_N) [b]	μ_{exp} (μ_N) [c]
^{91}Zr		$(d_{5/2})^1$	−1.44	−1.30
^{93}Mo	$(g_{9/2})^2$	$(d_{5/2})^1$	−1.42	−1.20
^{95}Mo	$(g_{9/2})^2$	$(d_{5/2})^3$	−0.95	−0.91
		$(g_{7/2})^2\ (d_{5/2})^1$	−1.53	
^{97}Mo	$(g_{9/2})^2$	$(d_{5/2})^5$	−0.50	−0.93
		$(g_{7/2})^2\ (d_{5/2})^3$	−1.07	
^{97}Ru	$(g_{9/2})^4$	$(d_{5/2})^3$	−0.93	−0.77
		$(g_{7/2})^2\ (d_{5/2})^1$	−1.51	
^{99}Ru	$(g_{9/2})^4$	$(d_{5/2})^5$	−0.50	−0.62
		$(g_{7/2})^2\ (d_{5/2})^3$	−1.05	
^{101}Ru	$(g_{9/2})^4$	$(g_{7/2})^2\ (d_{5/2})^5$	−0.61	−0.70
		$(g_{7/2})^4\ (d_{5/2})^3$	−1.16	

[a] Configuration above the core $^{90}_{40}Zr_{50}$.
[b] Calculated with parameters of Ref. 20.
[c] For references see Table II.

the Schmidt value ($\mu = -1.91\mu_N$) is probably due to the fact that the $\nu g_{9/2}$ shell is filled completely at $N = 50$, the $\nu g_{7/2}$ shell, however, is empty. Consequently, the $g_{9/2} \rightarrow g_{7/2}$ core polarization may be active, thus reducing the magnetic moments. For $N > 51$ the $d_{5/2} \rightarrow d_{3/2}$ excitations are responsible for a further reduction of μ. In a simple shell model picture the $d_{5/2}$ shell should be filled at $N = 56$, and thus, no $j^\pi = \frac{5}{2}^+$ ground-state configurations should be present for $N > 56$. It is experimentally found, however, that $j^\pi = \frac{5}{2}^+$ ground states occur up to $N = 61$ ($^{109}_{48}Cd_{61}$). This is due to the fact that the energy spacing between the $\nu d_{5/2}$ and $\nu g_{7/2}$ shell is relatively small, so that the filling of these two shells does not take place independently. In principle, the quasiparticle occupation probabilities u^2 and v^2 should be used for a proper description of the ground-state configurations. However, such data are not available with sufficient accuracy. Experimental values of magnetic moments of $\frac{5}{2}^+$ states can provide further information as a strong dependence of μ on the nuclear configuration is expected. Applying the core-polarization theory of Arima and Horie,[1] theoretical magnetic moments for the different extremal configurations are obtained. The result for ^{91}Zr, ^{93,95,97}Mo, and ^{97,99,101}Ru is listed in Table III. Although the absolute values are not described properly for ^{91}Zr and ^{93}Mo for which the neutron configuration is fixed, a similarity of the qualitative trend can be seen. For the Mo isotopes ^{93}Mo, ^{95}Mo, and ^{97}Mo the main neutron configuration is given by $(\nu d_{5/2})^1$, $(\nu d_{5/2})^3$, and $(\nu g_{7/2})^2\ (\nu d_{5/2})^3$, respectively. The main neutron configuration of the Ru isotopes ^{97}Ru, ^{99}Ru, and ^{101}Ru should then be $(\nu d_{5/2})^3$, $(\nu d_{5/2})^5$, and $(\nu g_{7/2})^2\ (\nu d_{5/2})^5$, respectively. The slight increase of the magnetic moments of the heaviest isotopes in these series is then explained consistently by the blocking of the $g_{9/2} \rightarrow g_{7/2}$ core polarization due to the more filled $\nu g_{7/2}$ shell. To investigate, whether the Pd isotopes fit into such a scheme, too, the magnetic moments of ^{101}Pd and ^{103}Pd would be interesting. NMR-ON measurements concerning this subject are in progress.

Moreover, our experiments have shown that the NMR-ON method is well suited for the precise determination of the hyperfine splitting constants of Ru*Fe* systems. The application to ^{103}Ru and ^{105}Ru could thus lead to a better understanding of the structure of these anomalous ground states.

ACKNOWLEDGMENTS

We want to thank Professor T. Yamazaki for discussions and Dr. P. Maier-Komor for the preparation of the Ru*Fe* alloys. We also thank the Gesellschaft für Kernforschung, Karlsruhe, for performing the neutron irradiations. This work was supported by the Bundesministerium für Forschung und Technologie.

[1]A. Arima and H. Horie, Prog. Theor. Phys. 12, 623 (1951).
[2]H. A. Mavromatis, L. Zamick, and G. E. Brown, Nucl. Phys. 80, 545 (1966); H. A. Mavromatis and L. Zamick, Nucl. Phys. A104, 17 (1967).
[3]H. Miyazawa, Prog. Theor. Phys. 6, 801 (1951).
[4]M. Chemtob, Nucl. Phys. A123, 449 (1969); M. Chemtob and M. Rho, *ibid.* A163, 1 (1971).
[5]S. Nagamiya, T. Katou, T. Nomura, and T. Yamazaki, Phys. Lett. 33B, 574 (1970); T. Yamazaki, in *Proceedings of the International Conference on Nuclear Structure and Spectroscopy, Amsterdam, 1974*, edited by H. P. Blok and A. E. L. Dieperink (Scholar's Press, Amsterdam, 1974), Vol. 2, p. 554 and references therein.
[6]E. Hagn, P. Kienle, and G. Eska, in *Proceedings of the International Conference on Nuclear Structure and Spectroscopy, Amsterdam, 1974*, edited by H. P. Blok and A. E. L. Dieperink (Scholar's Press, Amsterdam, 1974), Vol. 2, p. 576.
[7]O. Häusser, I. S. Towner, T. Faestermann, H. R. Andrews, J. R. Beene, D. Horn, D. Ward, and C. Broude, Nucl. Phys. A293, 248 (1977).
[8]J. Wese, E. Hagn, P. Kienle, and G. Eska (unpublished).
[9]S. R. de Groot, H. A. Tolhoek, and W. J. Huiskamp, *Alpha, Beta, and Gamma Ray Spectroscopy*, edited by K. Siegbahn (North-Holland, Amsterdam, 1965), Vol. 2, p. 1199.
[10]G. N. Rao, Nucl. Data Tables 15, 553 (1975).
[11]E. Matthias and R. J. Holiday, Phys. Rev. Lett. 17, 897 (1966).
[12]F. Bacon, J. A. Barclay, W. D. Brewer, D. A. Shirley, and J. E. Templeton, Phys. Rev. B 5, 2397 (1972).
[13]O. C. Kistner, Phys. Rev. 144, 1022 (1966).
[14]E. Matthias, S. S. Rosenblum, and D. A. Shirley, Phys. Rev. 139, B532 (1965).
[15]J. J. Murphy, T. J. Burch, and J. I. Budnick, J. Phys. Soc. Jpn. 36, 634 (1974).
[16]E. Hagn and G. Eska, in *Proceedings of the International Conference on Hyperfine Interactions Studied in Nuclear Reactions and Decay, Uppsala, Sweden, 1974*, edited by E. Karlsson and R. Wäppling (Uplands Grofiska AB, Uppsala, 1974), p. 148.
[17]M. Kopp and W. D. Brewer, Hyp. Int. 3, 321 (1978).
[18]E. Hagn, E. Zech, and G. Eska (unpublished).
[19]E. Hagn, E. Zech, and G. Eska, Hyp. Int. 4, 201 (1978).
[20]H. Noya, A. Arima, and H. Horie, Prog. Theor. Phys. Suppl. 8, 33 (1958).